

ARTICLES

On the nature of partial agonism in the nicotinic receptor superfamily

Remigijus Lape¹, David Colquhoun¹ & Lucia G. Sivilotti¹

Partial agonists are ligands that bind to receptors but produce only a small maximum response even at concentrations where all receptors are occupied. In the case of ligand-activated ion channels, it has been supposed since 1957 that partial agonists evoke a small response because they are inefficient at eliciting the change of conformation between shut and open states of the channel. We have investigated partial agonists for two members of the nicotinic superfamily—the muscle nicotinic acetylcholine receptor and the glycine receptor—and find that the open–shut reaction is similar for both full and partial agonists, but the response to partial agonists is limited by an earlier conformation change ('flipping') that takes place while the channel is still shut. This has implications for the interpretation of structural studies, and in the future, for the design of partial agonists for therapeutic use.

Agonists are small molecules that bind to a receptor and activate it. The best understood receptors are ligand-gated ion channels. When neurotransmitters bind to their extracellular domain, the resulting change of conformation opens an ion channel, which carries current through the cell membrane, allowing electrical signals to propagate. The natural neurotransmitters, acetylcholine and glycine, are very efficacious agonists: when they are bound, the channel is open for 95–98% of the time^{1,2}. In the 1950s, agonists were discovered that could not produce such a large response even when they saturated the binding sites. These were called partial agonists. Here we find that taurine can hold the glycine receptor channel open for at most about 54% of the time. del Castillo and Katz³ were the first to propose for an ion channel that when the receptor is occupied by a partial agonist the 'gating' equilibrium between open and shut conformations lies towards the shut side. This is equivalent to saying that agonists work because they have a higher affinity for the open state than the shut state^{4,5}, so their binding shifts the equilibrium towards the open state. The more efficacious the agonist, the greater is its selectivity for the open state. These views of partial agonism have persisted, essentially unchanged, for 50 years. However, recent findings suggest another possibility. Φ -value analysis indicates that, after binding, nicotinic receptors move through a number of brief intermediate shut states, a 'conformational wave', before the channel opens^{6–10}. Our own work on glycine receptors suggested that it is possible to detect and measure the properties of an intermediate conformation, which we refer to as 'flip'². The flipped receptor has a higher affinity for the agonist than the resting receptor, so it is a sort of activated, pre-open state. Higher affinity could result from domain closure around the bound agonist, a phenomenon that is clear in structures of extracellular domains of glutamate channels^{11,12}, but less obvious in the nicotinic superfamily^{13,14}, where binding sites are at the interface between subunits.

Here we investigate two partial agonists, taurine for glycine receptors, and tetramethylammonium (TMA) for nicotinic receptors. When our single-channel measurements are interpreted in terms of the flip mechanism, it is found that the open–shut reaction is remarkably similar for full and partial agonists. In both receptors, partial agonism originates from a reduced ability to flip, rather than a reduced ability to open. From the viewpoint of selective affinity, it is a low affinity for the flipped state, relative to the resting state, that

makes an agonist partial, rather than low affinity for the open state, relative to the resting state, as previously supposed. This interpretation places the root of partial agonism early in the chain of events that follow binding. It provides an experimental verification for Φ -value analysis^{6,9,10} as well as a functional counterpart for future structural measurements and it may be exploitable in rational drug design.

Results with the glycine receptor

Figure 1a shows raw single-channel data for three concentrations of a full agonist, glycine, and a partial agonist, taurine, on rat heteromeric $\alpha 1 \beta$ glycine receptors. At the highest concentrations it is obvious that the channel is open for more of the time with glycine than with taurine.

At 1–100 mM taurine, openings occurred in long clusters separated by long shut periods, presumably sojourns in long-lived desensitized states. Below 1 mM, openings were sparse and occurred in short bursts of openings separated by short shuttings (Fig. 1c).

The probability of being open, P_{open} (the fraction of time for which the channel is open; that is, the ratio between total open time per cluster and cluster length), reached a maximum of about 96% for glycine but only 54% for taurine (Fig. 1b). Unlike nicotinic channels, there was no sign of channel block by the agonist itself.

Plotting the distributions of apparent shut times ('apparent' means what is observed, as distorted by our inability to detect short events) shows that for both the partial agonist, taurine, and the full agonist, glycine, the mean lifetime of the brief shuttings is very similar, being between 10 and 14 μs , irrespective of concentration² (Fig. 1d).

To investigate what mechanisms might underlie our observations, we fitted putative mechanisms to the data with our HJCFT method. This method maximizes the likelihood of the entire sequence of openings and shuttings, with exact allowance for missed events. Simulation studies^{2,15} showed that this method is capable of estimating up to 18 rate constants with values as fast as 130,000 s^{-1} .

To estimate all the rate constants it is necessary to fit simultaneously a set of recordings at different agonist concentrations. First the mechanism to be tested must be postulated. We shall concentrate here on the flip mechanism (Fig. 2a) because it provides a realistic description of the wild-type glycine receptor² (see discussion below).

¹Department of Pharmacology, University College London, Medical Sciences Building, Gower Street, London WC1E 6BT, UK.

It was not possible to use taurine concentrations lower than 1 mM, for technical reasons described in Supplementary Information. Thus, it is not surprising that initial fits suggested that there were few monoligated openings in our records. Therefore monoligated flipped and open states were not included in the mechanism in the final fits (Fig. 2a, grey regions).

Figure 2 shows the results of a fit to a set of three records with 3, 10 and 100 mM taurine. It shows that the flip mechanism can, with a

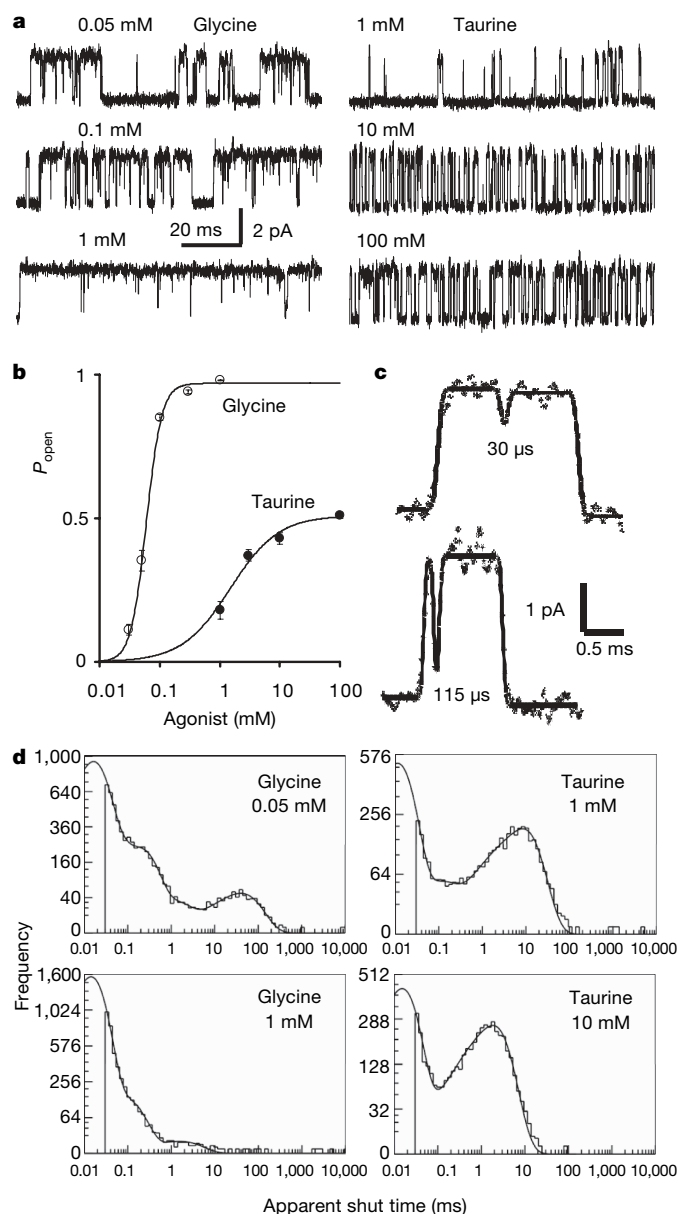


Figure 1 | Glycine channels show short interruptions when activated by either full or partial agonists. **a**, Single-channel currents (opening upwards) produced by a full agonist (glycine) or a partial agonist (taurine). **b**, Open probability increases with agonist concentration, reaching a maximum of 0.54 for taurine and 0.96 for glycine (17–60 clusters, 3–4 patches per point, \pm s.e.m.; Hill equation fits; glycine data from ref. 2). **c**, Short shut times are clearly detectable in channel activations by 1 mM taurine. Points are the digitized record and the continuous line is the best time-course fit obtained during idealization together with the estimated duration of the short gaps. **d**, Short shut times are the predominant component in shut-time distributions for both agonists. With the usual resolution of 30 μ s, a large proportion of such short shuttings are missed, but quite enough are observed to obtain a good estimate of their duration. Dwell-time distributions were fitted here and in Fig. 4b with a mixture of exponentials using EKDIST, so they are descriptive and not mechanism dependent.

single set of rate constants, predict well the observed open and shut times at all three concentrations and the observed P_{open} curve (continuous lines in Fig. 2b, c).

The average rate constants from nine recordings fitted as three independent sets (Table 1 and Supplementary Table 1) show that the opening rate for the fully liganded channel (β_3) is almost the same for the partial agonist, taurine, as it is for glycine. The shutting rate (α_3) is not greatly different from glycine either ($14,500 \text{ s}^{-1}$, compared with $7,000 \text{ s}^{-1}$), so the open–shut equilibrium constants ($E_3 = \beta_3/\alpha_3$) for taurine and glycine are similar (compared with a 180-fold difference in flipping equilibrium constants, Table 1). It has been assumed since 1957 (ref. 3) that partial agonism is a characteristic of the open–shut reaction but that is clearly not the case here. The major difference between taurine and glycine lies at an earlier stage, in the flipping reaction.

For glycine the equilibrium constant for flipping (F_3) is large (27) so most fully liganded receptors will adopt the pre-open flipped conformation. But for taurine this equilibrium constant is only

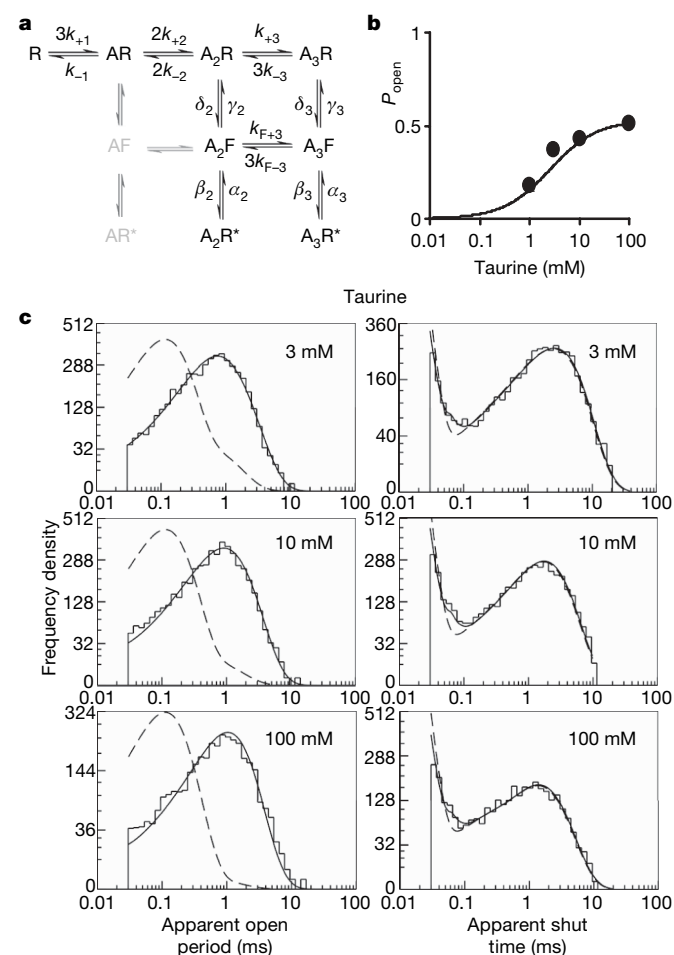


Figure 2 | Global fit of the taurine data with a flip mechanism provides a good description of the observations. **a**, The flip activation mechanism fitted by ref. 2 to $\alpha 1\beta$ channel activations by glycine. ‘A’ represents an agonist molecule; ‘R’ and ‘F’ represent the resting and flipped conformations of the receptor, respectively. The asterisk denotes an open channel. The success of the fit to the idealized records is judged by its ability to describe the experimental observations displayed in various ways¹⁵, as in **b** and **c**. The results of the fit predict accurately the channel open probability (**b**) and apparent open- and shut-time distributions at all concentrations as shown by the continuous lines (fit predictions) superimposed onto the data points and the histograms. The dashed lines in the histograms are the distributions predicted if the records were obtained with perfect resolution (that is, no events were missed; for full data display see Supplementary Fig. 1 and Supplementary Table 1).

Table 1 | Summary of results with full and partial agonists

	Glycine	Taurine	Acetylcholine (−100 mV)	Acetylcholine (+80 mV)	TMA (−80 mV)	TMA (+80 mV)
E_2	-	-	34.4	3.1	28.1	2.8
F_2	-	-	3.8	1.1	0.14	0.060
E_3	20	9.2	-	-	-	-
F_3	27	0.15	-	-	-	-
K (μM)	520	1,040	40.1	43	3,000	2,310
K_F (μM)	8	690	20.7	0.13	340	1,240
α_2 (s ⁻¹)	-	-	2,560	9,550	2,520	9,100
β_2 (s ⁻¹)	-	-	87,700	29,400	70,500	25,000
α_3 (s ⁻¹)	7,000	14,500	-	-	-	-
β_3 (s ⁻¹)	129,000	133,000	-	-	-	-

For estimates of all rate constants, and their errors, and more complete tests of fit, see Supplementary Information. K and K_F are dissociation equilibrium constants for the resting and flipped conformations, respectively.

0.15, so 87% of fully liganded shut receptors will be in the resting conformation, not in the flipped, pre-open conformation. This is summarized in Fig. 3. A schematic representation of the three states (resting, flipped and open) visited by the fully liganded receptor is shown in Fig. 3a. The rates of transition between states are indicated by the size of the arrows (Fig. 3b), for glycine and taurine. The open–shut transition is similar for both agonists. Another way to look at that is through the energy diagram in Fig. 3c, in which the paths for the open–shut transition almost superimpose. The energy diagram shows also that the transition from resting to flipped state is downhill for glycine but uphill for taurine. The overall energy change, from resting to open state, is downhill for glycine, but nearly level for taurine, as expected because the channel is open for about half the time in saturating taurine. In the case of taurine, the transition from resting to flipped is slow, so the mean lifetime of the saturated resting state is much longer than for glycine (Fig. 3b; see also animation in Supplementary Information) and this is why taurine is a partial agonist.

Another way to look at this result is that the effectiveness of an agonist depends largely on its relative affinity for resting and flipped conformations, rather than, as previously supposed, its relative affinity for resting and open conformations. Glycine binds with 65-times greater affinity to the flipped conformation than to the resting state, but taurine binds only slightly (about 1.5-fold) more tightly. Most of this difference arises from the lower affinity of taurine for the flipped state.

Results with the nicotinic receptor

Figure 4a depicts cell-attached activations of human muscle nicotinic receptor elicited by the full agonist acetylcholine (−100 mV transmembrane potential) and by the partial agonist TMA (−80 and +80 mV).

At negative membrane potentials, an acetylcholine-activated channel is practically always open at saturating agonist concentrations (94% of the time), whereas a TMA-bound channel can open for only 78% of the time (Fig. 4c).

TMA recordings showed many brief shuttings, which resemble closely those seen with the full agonist, acetylcholine (mean duration about 13 μs at negative potentials¹) (Fig. 4b). The time constant of the fastest component did not vary noticeably with TMA concentration, but was briefer at negative (12.8 ± 0.46 μs, 13 patches) than at positive (27.9 ± 1.9 μs; 7 patches) membrane potentials. Brief shuttings cannot be attributed entirely to channel block because they were frequent at positive as well as at negative membrane potentials.

Figure 4d shows an important difference between nicotinic and glycine receptors. At negative potentials the amplitude of the openings appears to decrease progressively as agonist concentration increases. This is because in nicotinic receptors the agonist can bind to a second, lower affinity site in the channel pore and produce fast block. Both openings and blockages are very brief and failure to resolve them results in the apparent decrease in channel amplitude (equilibrium constant for TMA block, K_B , 8.9 ± 0.6 mM). At

+80 mV there is little or no block, as expected^{16–18}: channel amplitude is not affected by TMA concentrations as high as 100 mM, the highest on our P_{open} curve. At +80 mV both agonists are less efficacious than at negative potentials: a fully TMA-bound channel opens only for 16% of the time compared with 59% for acetylcholine (Fig. 4a, c and Supplementary Fig. 3).

The original motive for the flip mechanism was to describe in a physically plausible way the apparent strong interaction between binding sites in glycine receptors when conventional mechanisms were fitted². That sort of apparent interaction is much less pronounced for the nicotinic receptor. Nevertheless the flip mechanism fitted nicotinic data well, and it has the virtue of obviating the need to add arbitrary shut states in order to get a good fit^{1,19}.

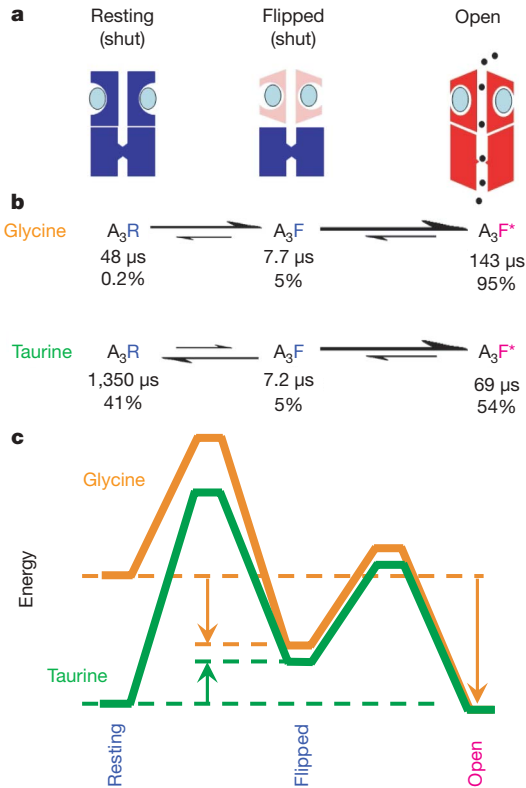


Figure 3 | Activation of the glycine channel by the full agonist glycine and the partial agonist taurine. **a**, The three states of the fully saturated receptor. The resting (shut) channel changes conformation to reach a partially activated state (flipped), still shut, but with increased affinity for the agonist (blue ellipses). It is from this flipped state that the channel can open (red, right). **b**, The reaction rates for channel activation by glycine and taurine differ largely in the first step, the flipping. Relative rates are indicated by the size of arrows. The diagram shows also the mean lifetime of each state (μs) and the proportion of time (percentage) spent by a bound channel in each of the states at equilibrium. A channel occupied by glycine doesn't stay long in the resting state, but quickly flips. When taurine is bound, the channel takes a long time to flip, so it spends much more time in the closed resting state. Once the channel has reached the flipped intermediate state, it opens quickly, regardless of which agonist is bound. The probability of opening, rather than unflipping, is over 96% for both agonists, so a burst of many openings results. **c**, An energy diagram for the three states of the saturated receptor, for full agonist (glycine, orange) and partial agonist (taurine, green). Again, the difference lies largely in the resting–flipped transition. As indicated by arrows, the transition from resting to flipped is downhill for glycine, but uphill for taurine. The overall transition from resting to open is very downhill for glycine, but almost level for taurine, as expected from the maximum response of about 54% open. The calculations used a frequency factor²⁷ of 10⁷ s⁻¹ and the lines are shifted vertically so that they meet at the open state. (See also Supplementary Movie.)

Figure 5 shows part of the results of fitting TMA records with the mechanism in Fig. 5a (see also Supplementary Figs 4 and 5 and Table 1). At -80 mV the largest TMA concentration used for fits was 30 mM because channel block became too pronounced at higher concentrations (Fig. 4d). Again the distributions of apparent dwell times and the P_{open} curve are predicted well by the results of the fit (Fig. 5b, c).

The fully liganded opening rate (β_2) at -80 mV is about $71,000 \text{ s}^{-1}$, very similar to the value for acetylcholine ($88,000 \text{ s}^{-1}$).

The shutting rates also are almost identical, with $\alpha_2 = 2,560 \text{ s}^{-1}$ for acetylcholine and $2,520 \text{ s}^{-1}$ for TMA. Consequently, the fully liganded gating constant, E_2 , is similar for acetylcholine and TMA. Again, what differs between full and partial agonist is the flipping step. For acetylcholine the flipping equilibrium constant, F_2 , is 3.8 but for TMA it is only 0.14, so TMA has a far smaller ability to elicit the pre-open flipped state than acetylcholine, and that is why it is a partial agonist.

It is important to rule out the possibility that these results could be influenced by channel block because at the highest TMA concentration

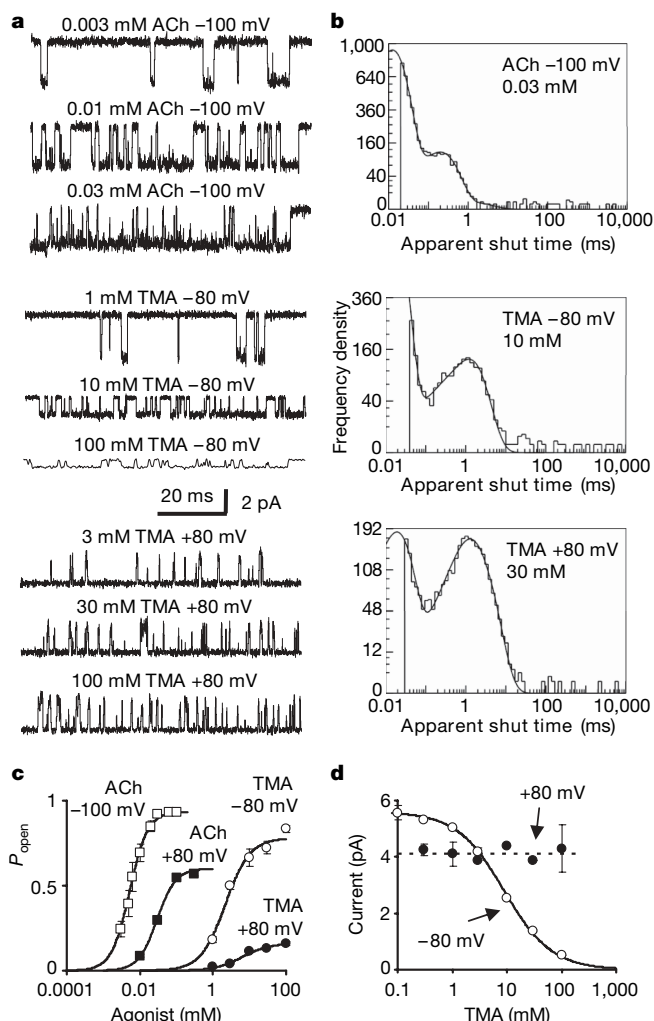


Figure 4 | Short interruptions in openings of muscle nicotinic channels occur with both partial and full agonists and cannot be attributed entirely to channel block. **a**, Single channel currents produced by a full agonist (acetylcholine) and a partial agonist (TMA, openings downwards in the first six rows). ACh, acetylcholine. **b**, Short shut times are a major feature of shut-time distributions irrespective of agonist, voltage and concentration (see Supplementary Figs 2 and 4). Some of these brief shuttings could result from fast open-channel block at negative potentials, but not at positive potential, when open-channel block is essentially absent. **c**, Open probability reaches a maximum of $0.94 (\pm 0.004)$ for acetylcholine at -100 mV but is lower (0.59 ± 0.01) for acetylcholine at $+80$ mV and for TMA at -80 or $+80$ mV (0.78 ± 0.05 or 0.16 ± 0.02 , respectively) (2–4 patches per point, \pm s.e.m.; Hill equation fits). These fits give also: for acetylcholine -100 mV, concentration for 50% of maximum response (EC_{50}) = $5.3 \pm 0.2 \mu\text{M}$ and Hill coefficient (n_H) = 1.7 ± 0.1 ; for acetylcholine $+80$ mV, EC_{50} = $29 \pm 2 \mu\text{M}$ and n_H = 1.7 ± 0.1 ; for TMA -80 mV, EC_{50} = $2.2 \pm 0.5 \text{ mM}$ and n_H = 1.3 ± 0.4 ; and for TMA $+80$ mV, EC_{50} = $6.4 \pm 1.9 \text{ mM}$ and n_H = 1.2 ± 0.4 . **d**, Because of open-channel block, the amplitude of single-channel currents declines with increasing TMA concentrations at negative potentials (open circles), but not at positive transmembrane potentials (filled circles, 2–3 patches per point, \pm s.e.m.).

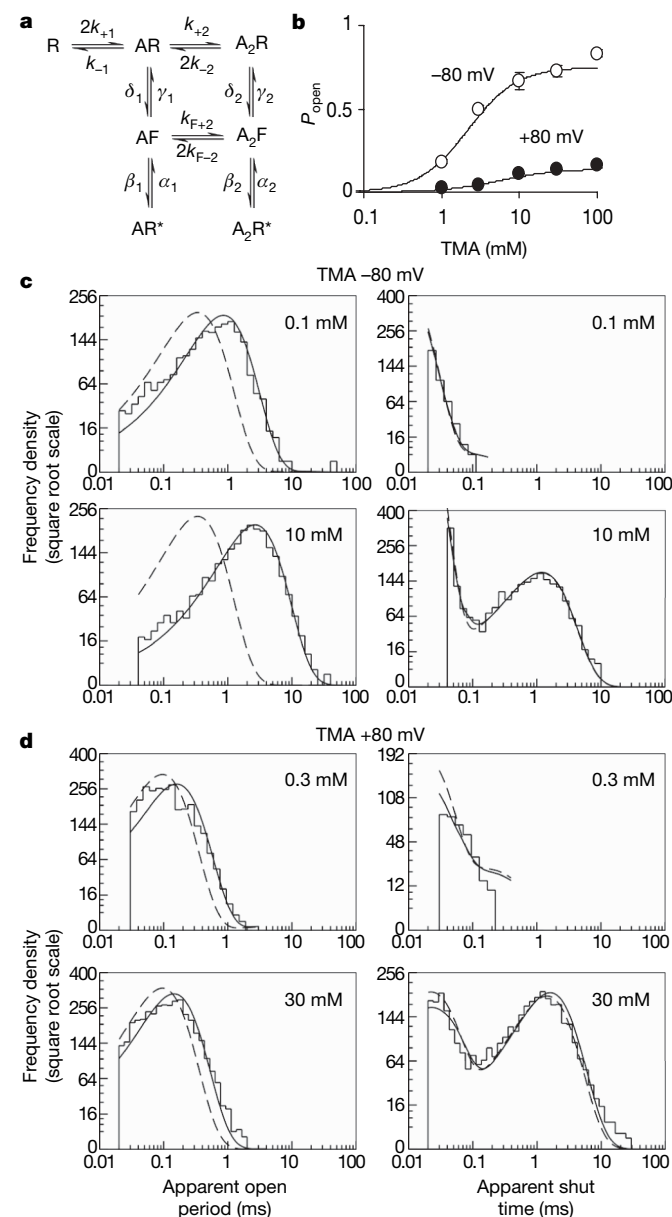


Figure 5 | The flip mechanism describes well the activation of acetylcholine receptors by TMA. **a**, Schematic representation of the flip mechanism used here: this has two agonist binding sites. As in Fig. 2, the experimental data are displayed as channel open probability values (\pm s.e.m.) in **b** or dwell-time distributions in **c**, **d**. The results of fitting the idealized records are used to calculate the predicted P_{open} —concentration curves and distributions (continuous lines). Both the open probability values and the dwell time distributions are well described by the fitted rate constants for TMA, at both -80 mV (**c**) and $+80$ mV (**d**). The dashed lines in the histograms are the distributions predicted if the records were obtained with perfect resolution (that is, no events were missed). The full data display for the fits for acetylcholine and TMA is in Supplementary Figs 2, 4 and 5 and Supplementary Table 2.

fitted (10 mM), channels are blocked for about half the time at -80 mV. The experiments were therefore repeated at positive membrane potential, $+80$ mV, where block is essentially absent (Fig. 4d). Short shuttings are still present at positive membrane potentials, so they cannot all be caused by brief channel blockages. The open–shut equilibrium constant is reduced about tenfold at $+80$ mV (Table 1), so acetylcholine itself becomes a partial agonist¹⁸ (Fig. 4c and Supplementary Fig. 3). The maximum P_{open} for acetylcholine is reduced from 94% at -100 mV to about 60% at $+80$ mV and the maximum P_{open} for TMA is reduced from 78% to 16%. So TMA is still much less efficacious than acetylcholine when the complication of block is removed, and for exactly the same reason. The open–shut equilibrium constant for TMA at $+80$ mV ($E_2 = 2.8$) is almost the same as that for acetylcholine ($E_2 = 3.1$), but again the flipping equilibrium constant for TMA, F_2 , is very small, only 0.06, almost 20-fold less than for acetylcholine, so this remains the reason why TMA is a partial agonist.

Discussion

Our analysis of single-channel data suggests that in the nicotinic superfamily partial agonism is not, as has been supposed for 50 years, a property of the open–shut transition, but arises in the earlier conformation change from the resting state to an intermediate pre-open (or ‘activated’) conformation dubbed the flip state. The same conclusion was reached for two members of this superfamily: the nicotinic acetylcholine receptor and the heteromeric glycine receptor. Figure 3 represents schematically the states visited by the agonist-bound channel during activation and summarizes our quantitative findings for the glycine receptor.

The conclusion that the final step in activation, channel opening, is much the same for full and partial agonists comes from the observation that both partial and full agonists produce similar brief shuttings (7–8 μ s on average for both glycine and taurine). It has been supposed since 1981 (refs 20, 21) that these brief closures are mostly oscillations between the open state and the immediately preceding fully liganded shut state (here the flipped intermediate), and therefore reflect the properties of the open–shut reaction. The similarity in the open–shut transition for the two agonists is obvious from the fact that the energy profile for this step is almost identical for glycine and taurine (Fig. 3c).

It has been known for a long time²² that the conductance of single channels is the same whichever agonist activates them. It is intriguing that we now find that not only the conductance but also the opening and shutting rate of channels do not vary greatly between full and partial agonists in the nicotinic superfamily.

The maximum P_{open} response that can be obtained has always been assumed to depend only on the equilibrium constant for the open–shut step (E), being $E/(1 + E)$ (ref. 23). In the context of the flip mechanism, the maximum response depends not only on E but also on the equilibrium constant for flipping, F . The maximum P_{open} becomes $E_{\text{eff}}/(1 + E_{\text{eff}})$, where $E_{\text{eff}} = EF/(1 + F)$. Here this effective gating constant, E_{eff} , is about 19 for glycine but only 1.2 for taurine, largely because F is lower for the partial agonist. For taurine, the early conformational step is uphill energetically (green arrow in Fig. 3c), and it is much slower than it is for glycine (illustrated by the size of the arrows in Fig. 3b; Supplementary Table 1). The equilibrium between resting and flipped favours the resting state, in which taurine-bound channels spend much more time (on average 1,350 μ s) than glycine-bound channels (48 μ s).

Our interpretation places the origin of partial agonism at an earlier stage in the activation process than before. This is entirely consistent with the conclusion of a previous study⁶, in which the analysis of linear free-energy relationships implied that the differences between nicotinic agonists lie early in the activation process, quite close to the transmitter binding site. Indeed calculation of the Φ value for the overall resting-to-open transition gives a value close to 1, as that study found⁶ (Supplementary Information). Our result also explains

the observation that the conformation change close to the membrane, in the M2–M3 region, appears to be similar for both glycine and taurine, as judged by the reaction rate with a cysteine-reactive compound²⁴.

We may speculate that flipping corresponds to the domain closure around the bound agonist seen in the extracellular domain of glutamate channels and, to a lesser extent, in the acetylcholine binding protein^{11–14}. This structural work cannot be compared directly with our results because it all comes from non-functional receptors, does not tell us how fast domain closure is, how it changes agonist affinity in the intact channel or how it relates to channel opening.

Our single-channel work allowed us to obtain a functional characterization of a partially activated intermediate state, to measure exit and entry rates into this state and its average lifetime with different agonists in two nicotinic superfamily channels. This finding will constrain and inform computational simulations of the dynamics of channel activation and influence the interpretation of structural studies. In addition to that, our findings may also help reinterpret earlier mutation studies, as the greater detail of our model now shows that what was called ‘affinity for the resting state’ may reflect also the higher affinity for a partially activated intermediate. This could perhaps account for the awkward observation that some mutations that are nowhere near the binding site nevertheless appear to affect largely the agonist binding to the resting state²⁵. Another implication testable by structural data is that partial and full agonists should differ in their interaction with the portion of the binding site that moves during domain closure.

METHODS SUMMARY

Cell-attached single-channel currents were recorded from HEK293 cells expressing²⁶ human adult muscle nicotinic receptors or rat $\alpha 1\beta$ glycine receptors.

Rate constant values were estimated by direct model fitting to sets of records idealized by time-course fitting (HJCFT and SCAN programs, respectively; <http://www.ucl.ac.uk/Pharmacology/dc.html>).

Full Methods and any associated references are available in the online version of the paper at www.nature.com/nature.

Received 24 April; accepted 5 June 2008.

Published online 16 July 2008.

1. Hatton, C. J., Shelley, C., Brydson, M., Beeson, D. & Colquhoun, D. Properties of the human muscle nicotinic receptor, and of the slow-channel myasthenic syndrome mutant ϵ L221F, inferred from maximum likelihood fits. *J. Physiol.* **547**, 729–760 (2003).
2. Burzomato, V., Beato, M., Groot-Kormelink, P. J., Colquhoun, D. & Sivilotti, L. G. Single-channel behavior of heteromeric $\alpha 1\beta$ glycine receptors: An attempt to detect a conformational change before the channel opens. *J. Neurosci.* **24**, 10924–10940 (2004).
3. del Castillo, J. & Katz, B. Interaction at end-plate receptors between different choline derivatives. *Proc. R. Soc. Lond. B* **146**, 369–381 (1957).
4. Wyman, J. & Allen, D. W. The problem of the heme interactions in hemoglobin and the basis of the Bohr effect. *J. Polym. Sci. C* **7**, 499–518 (1951).
5. Grosman, C., Zhou, M. & Auerbach, A. Mapping the conformational wave of acetylcholine receptor channel gating. *Nature* **403**, 773–776 (2000).
6. Chakrapani, S., Bailey, T. D. & Auerbach, A. Gating dynamics of the acetylcholine receptor extracellular domain. *J. Gen. Physiol.* **123**, 341–356 (2004).
7. Zhou, Y., Pearson, J. E. & Auerbach, A. ϕ -value analysis of a linear, sequential reaction mechanism: theory and application to ion channel gating. *Biophys. J.* **89**, 3680–3685 (2005).
8. Auerbach, A. Gating of acetylcholine receptor channels: brownian motion across a broad transition state. *Proc. Natl Acad. Sci. USA* **102**, 1408–1412 (2005).
9. Purohit, P., Mitra, A. & Auerbach, A. A stepwise mechanism for acetylcholine receptor channel gating. *Nature* **446**, 930–933 (2007).
10. Armstrong, N., Sun, Y., Chen, G. Q. & Gouaux, E. Structure of a glutamate-receptor ligand-binding core in complex with kainate. *Nature* **395**, 913–917 (1998).
11. Jin, R., Banke, T. G., Mayer, M. L., Traynelis, S. F. & Gouaux, E. Structural basis for partial agonist action at ionotropic glutamate receptors. *Nature Neurosci.* **6**, 803–810 (2003).
12. Celie, P. H. et al. Nicotine and carbamylcholine binding to nicotinic acetylcholine receptors as studied in AChBP crystal structures. *Neuron* **41**, 907–914 (2004).
13. Hansen, S. B. et al. Structures of aplysia AChBP complexes with nicotinic agonists and antagonists reveal distinctive binding interfaces and conformations. *EMBO J.* **24**, 3635–3646 (2005).

15. Colquhoun, D., Hatton, C. J. & Hawkes, A. G. The quality of maximum likelihood estimates of ion channel rate constants. *J. Physiol.* **547**, 699–728 (2003).
16. Adams, P. R. Voltage jump analysis of procaine action at frog end-plate. *J. Physiol.* **268**, 291–318 (1977).
17. Neher, E. & Steinbach, J. H. Local anaesthetics transiently block currents through single acetylcholine-receptor channels. *J. Physiol.* **277**, 153–176 (1978).
18. Colquhoun, D. & Ogden, D. C. Activation of ion channels in the frog end-plate by high concentrations of acetylcholine. *J. Physiol.* **395**, 131–159 (1988).
19. Salamone, F. N., Zhou, M. & Auerbach, A. A re-examination of adult mouse nicotinic acetylcholine receptor channel activation kinetics. *J. Physiol.* **516**, 315–330 (1999).
20. Colquhoun, D. & Sakmann, B. Fluctuations in the microsecond time range of the current through single acetylcholine receptor ion channels. *Nature* **294**, 464–466 (1981).
21. Colquhoun, D. & Sakmann, B. Fast events in single-channel currents activated by acetylcholine and its analogues at the frog muscle end-plate. *J. Physiol. (Lond.)* **369**, 501–557 (1985).
22. Gardner, P., Ogden, D. C. & Colquhoun, D. Conductances of single ion channels opened by nicotinic agonists are indistinguishable. *Nature* **309**, 160–162 (1984).
23. Colquhoun, D. Binding, gating, affinity and efficacy. The interpretation of structure-activity relationships for agonists and of the effects of mutating receptors. *Br. J. Pharmacol.* **125**, 923–948 (1998).
24. Han, N. L., Clements, J. D. & Lynch, J. W. Comparison of taurine- and glycine-induced conformational changes in the M2–M3 domain of the glycine receptor. *J. Biol. Chem.* **279**, 19559–19565 (2004).
25. Colquhoun, D., Unwin, N., Shelley, C., Hatton, C. & Sivilotti, L. G. *Drug Discovery and Drug Development* (ed. Abrahams, D.) 357–405 (John Wiley, New York, 2003).
26. Groot-Kormelink, P. J., Beato, M., Finotti, C., Harvey, R. J. & Sivilotti, L. G. Achieving optimal expression for single channel recording: a plasmid ratio approach to the expression of $\alpha 1$ glycine receptors in HEK293 cells. *J. Neurosci. Methods* **113**, 207–214 (2002).
27. Andersen, O. S. Editorial: Graphic representation of the results of kinetic analyses. *J. Gen. Physiol.* **114**, 589–590 (1999).

Supplementary Information is linked to the online version of the paper at www.nature.com/nature.

Acknowledgements This work was supported by grants from the MRC (Programme grant G0400869) and the Wellcome Trust (Project grant 074491) to L.G.S. and D.C. We are grateful to F. Abogadie for molecular biology, to I. Vais for programming help, and to D. Jane for purification of taurine.

Author Information Reprints and permissions information is available at www.nature.com/reprints. Correspondence and requests for materials should be addressed to D.C. (d.colquhoun@ucl.ac.uk).

METHODS

Single-channel electrophysiology. Cell-attached single-channel currents were recorded at 19–21 °C from HEK293 cells transiently transfected by a Ca^{2+} -phosphate co-precipitation method²⁶ with pcDNA3.1 plasmids coding for human muscle acetylcholine nicotinic receptor subunits ($\alpha 1$, β , δ , ϵ , ratio 2:1:1:1) or rat heteromeric glycine receptor subunits ($\alpha 1$, β , ratio 1:1 or 1:4), together with plasmid coding for eGFP. The pipette solution was freshly prepared by diluting agonist stocks with extracellular solution which contained (in mM): 5.4 NaCl, 142 KCl, 1.8 CaCl_2 , 1.7 MgCl_2 and 10 HEPES (pH adjusted to 7.4 with KOH) for acetylcholine receptor experiments or, for glycine receptor experiments, 102.7 NaCl, 20 Na gluconate, 4.7 KCl, 2 CaCl_2 , 1.2 MgCl_2 , 10 HEPES, 14 glucose, 15 sucrose, 20 TEA-Cl (pH adjusted to 7.4 with NaOH). Osmolarity was 320 mOsm for all solutions.

Taurine (Fluka) was found by an HPLC assay to be contaminated by glycine (3 parts in 100,000, molar ratios). It was, therefore, purified before use (by D. Jane). Taurine was passed through an ion exchange resin column, followed by crystallization from the water eluate. This purification was found to be essential to avoid glycine-induced openings in recordings made at high taurine concentrations.

Patch pipettes were made from thick-walled borosilicate glass (GC150F, Harvard Instruments) and coated near the tip with Sylgard 184 (Dow Corning). Electrode resistance was in the range 8–15 M Ω after fire-polishing. Single-channel currents were recorded with an Axopatch 200B amplifier (Axon Instruments), filtered at 10 kHz (sampling rate 100 kHz) and stored on the PC hard drive.

Pipette potential was held at +100 mV for the glycine experiments and at +100, –80 or +80 mV for the nicotinic experiments.

Analysis. For off-line analysis, data were filtered at 3–8 kHz and sampled at 33–100 kHz. Records were idealized by time-course fitting (SCAN program; <http://www.ucl.ac.uk/Pharmacology/dc.html>), and the appropriate resolution (20–100 μs) was imposed before fitting dwell-time distributions with mixtures of exponential probability densities (EKDIST program). Rate constant values were estimated by direct model fitting to the idealized records (HJCFIT program). This was performed on sets of experiments, each set containing three (four for acetylcholine) agonist concentrations spanning the dose–response curve from the minimum concentration that elicited clusters of openings (that could be attributed to a single molecule) to the maximum P_{open} . Each experiment contained 10,000–20,000 transitions. Fits were repeated, systematically changing initial guesses to ensure that the convergence was to a global maximum of the likelihood surface.

On the nature of partial agonism in the nicotinic receptor superfamily

Remigijus Lape, David Colquhoun & Lucia G. Sivilotti

Animated version of Figure 3a,b

A movie animation (flip-movie.wmv) can be downloaded. The first part illustrates transitions between the three states of the receptor that exist in a saturating concentration of glycine (see Fig 3a). The second part shows the same for taurine. The speed is slowed down by a factor of 10,000 (1 second per 100 μ s), and is realistic apart from the fact that channels will re-open more times than is shown before reverting to the shut state. The animation shows that the smaller maximum response for taurine, compared with glycine, results mainly from the longer sojourns in the resting conformation (A_3R) with taurine, because of the slower transition rate from the resting conformation (A_3R) to the flipped (A_3F). Once the flipped conformation is reached, bursts of openings occur that are very similar for both agonists.

METHODS***Cell culture and transfection of cells.***

Human embryonic kidney (HEK293) cells, obtained from the American Type Culture Collection (ATCC), were cultured and maintained in Dulbecco's modified Eagle medium containing 10% (v/v) foetal bovine serum and 1% (v/v) penicillin streptomycin solution (10,000 units/ml penicillin and 10 mg/ml streptomycin; all from Gibco, UK) at 37°C. Before experiments, cells were plated onto polylysine-coated coverslips in 35 mm culture dishes and transfected by a Ca^{2+} -phosphate co-precipitation method¹. The DNA consisted of pcDNA3.1 plasmids (Invitrogen, The Netherlands) containing inserts encoding the human adult muscle acetylcholine receptor subunits $\alpha 1$, $\beta 1$, δ , ϵ , rat glycine receptor subunits $\alpha 1$, β (GenBank accession numbers Y00762, X14830, X55019, X66403, AJ310834 and AJ310839, respectively), enhanced green fluorescent protein (eGFP; Clontech, UK) or no insert (non-coding plasmid). The mixture of DNA used for the cell transfection contained 5% acetylcholine receptor subunit DNA ($\alpha 1$, $\beta 1$, δ , ϵ ratio 2:1:1:1), 65% eGFP DNA, and 30% non-coding plasmid or 16% glycine receptor subunit DNA ($\alpha 1$, β ratio either 1:4 or 1:1), 30% eGFP DNA, and 65% non-coding plasmid. Each cell culture dish was transfected with a total amount of 3 μ g of DNA.

In order to avoid contamination of recordings with homomeric glycine receptors, it is necessary to transfect cells with a large excess of β subunit DNA², but we found that this frequently resulted in

receptors that were heterogeneous at the single channel level. Receptors were more homogeneous when less β subunit DNA was used, so transfections were done with 1:1 or 1:4 ratio of $\alpha 1$ to β subunit DNA. This, though essential, meant that records contained variable proportions of homomeric $\alpha 1$ channels. Contaminant homomeric channels can be distinguished from heteromeric receptors because of their higher conductance^{3,4}. However this restricted us to the higher end of the concentration range where clusters of openings from one individual channel occurred. At lower concentrations there were many isolated openings that were too short for their amplitude to be measured unambiguously.

Single channel recordings and analysis.

All recordings were performed in the cell-attached configuration using acetylcholine (ACh), tetramethylammonium (TMA) or taurine as acetylcholine receptor or glycine receptor agonists in the pipette. For recording acetylcholine receptor single-channel currents, the extracellular solution contained (mM): 5.4 NaCl, 142 KCl, 1.8 CaCl₂, 1.7 MgCl₂ and 10 HEPES (pH adjusted to 7.4 with KOH). The pipette solution was made just before recording by mixing a stock solution containing (mM) 5.4 NaCl, 142 KCl, 1.8 CaCl₂, 1.7 MgCl₂, 10 HEPES and 100 TMA or ACh (pH adjusted to 7.4 with KOH) with standard extracellular solution to obtain the required agonist concentration. For recording glycine receptor single channel currents, the extracellular solution contained (mM): 102.7 NaCl, 20 Na gluconate, 4.7 KCl, 2 CaCl₂, 1.2 MgCl₂, 10 HEPES, 14 glucose, 15 sucrose, 20 TEA-Cl (pH adjusted to 7.4 with NaOH). Just before recording, the pipette solution was prepared by mixing a stock (mM): 85 NaCl, 4.7 KCl, 2 CaCl₂, 1.2 MgCl₂, 10 HEPES, 20 TEA-Cl and 100 taurine (pH adjusted to 7.4 with NaOH) with standard extracellular solution. For the glycine receptor experiments we used HPLC-grade water (HiPerSolv, VWR, UK) in order to reduce glycine contamination. Osmolarity was 320 mOsm for all solutions.

Taurine (Fluka) was found by an HPLC assay to be contaminated by glycine (3 parts in 100,000, molar ratios). It was, therefore, purified before use (by Dr David Jane, Pharmacology Dept, University of Bristol). Taurine was passed through an ion exchange resin column, followed by crystallisation from the water eluate. This purification was found to be essential to avoid glycine-induced openings in recordings made at high taurine concentrations.

Patch pipettes were made from thick-walled borosilicate glass (GC150F, Harvard Instruments) and coated near the tip with Sylgard 184® (Dow Corning). Electrode resistance was in the range 8-15 M Ω after fire-polishing. Single-channel currents were recorded with an Axopatch 200B amplifier

(Axon Instruments, California, USA), filtered at 10 kHz (sampling rate 100 kHz) and stored on the PC hard drive.

In the nicotinic receptor experiments, the high K^+ ion concentration in the extracellular solution (142 mM) means that the cell resting potential is expected to be near to 0 mV. Thus, the transmembrane potential of the patch during recording is approximately equal to the absolute value of the holding potential but of opposite sign. In the glycine receptor experiments, the cell resting potential is not artificially depolarised as the extracellular K^+ concentration is 4.7 mM, hence the real patch transmembrane potential during recording will be more negative than -100 mV (i.e. -100 mV plus the resting membrane potential of the HEK293 cell, typically between -20 and -40 mV⁵). The observed amplitude of the currents for heteromeric receptors for taurine was 2.9 ± 0.1 pA ($n = 14$), much the same as for glycine (3.1 pA⁶).

We did not correct for junction potential, as with our solutions this is expected to be at most 1 mV (as calculated in Clampex 9, Axon Instruments). All experiments were done at $19 - 21^\circ\text{C}$.

For off-line analysis, data were filtered at $3 - 8$ kHz and sampled at $33 - 100$ kHz. Open times, shut times, and amplitudes were idealized with SCAN (<http://www.ucl.ac.uk/pharmacology/dc.html>) and dwell-time distributions were fitted with mixtures of exponential densities using the EKDIST program after imposing a resolution of $20\text{--}100$ μs . For each recording, $10,000\text{--}20,000$ transitions were fitted.

Because we do not know the number of channels in the patch, it is essential for model fitting to divide the idealised single channel record into stretches that originate, almost certainly, from one individual channel. When openings are sparse (at low agonist concentrations) such stretches are short, each consisting of a single activation (short burst of openings) of the channel, but when P_{open} is high, long stretches of data with no second channel opening can be obtained. The division of the record into one-channel stretches was achieved by defining a critical shut time, t_{crit} , on the basis of inspection of the shut time distribution. Sometimes this process can be ambiguous but our conclusions do not depend critically on this choice. The shut time distributions are shown only up to t_{crit} , because shut times longer than this were not used for fitting.

Selection of data records

Recordings made at different concentrations of agonist were grouped arbitrarily into sets for simultaneous fitting. Each set included one recording at each of the concentrations used (four for

ACh at -100 mV, three for all other agonists) and the sets were independent, i.e. each individual patch was included in only one set. The data reported here are the result of fitting three such replicate sets (two for ACh and TMA at +80 mV). Records that showed obvious heterogeneity, as judged mainly by occurrence of clusters of openings with abnormally high P_{open} , were excluded. Two recordings (one for ACh and one for TMA) were excluded on the grounds that they gave values for association rate constants greater than $10^9 \text{ M}^{-1}\text{s}^{-1}$, a value that is physically impossible. The temporal resolution of TMA-activated single-channel records at negative transmembrane potential rapidly worsened at concentrations higher than 1 mM as the reduction in the apparent channel amplitude (Fig. 4a) meant that a progressively larger fraction of short closings was missed.

The main conclusion, that partial agonists showed a low flipping constant (F) rather than a low gating constant (E), was insensitive to the choice of which sets to exclude. The less well-defined constants that refer to receptors that are not fully-liganded were rather more sensitive, but their exact values are not crucial for our argument.

Allowance for channel blocking action in fits of acetylcholine and TMA data at negative membrane potentials

Both nicotinic agonists produced channel block at negative potentials. The fact that we get very similar results at positive membrane potentials where block is essentially absent rules out channel block as an explanation for our results, but it is necessary to consider its effect at negative potentials.

The case of ACh is the simplest. With ACh as agonist, the channel blockages are sufficiently long that some of them can be detected. The blocked state (A_2R*B in Supplementary Fig. 2) can therefore be included as a discrete state and the association and dissociation rate constants for the open channel block fitted as free parameters. The results are shown in Supplementary Table 2. The association rate constant, k_{+B} , was $8.6 \times 10^7 \text{ M}^{-1}\text{s}^{-1}$ and the dissociation rate constant implied a mean blockage length of 10 μs .

TMA is somewhat more difficult, because essentially all the channel blockages that it produces seem to be too short to be resolved. Figure 4d shows that at the highest TMA concentration fitted (10 mM), channels are blocked for about half the time at -80 mV, because the apparent channel amplitude is approximately halved. If we assume the simplest mechanism (pure open channel block) and we make the reasonable supposition that the association rate constant for TMA block is

similar to that measured for ACh ($8.6 \times 10^7 \text{ M}^{-1} \text{ s}^{-1}$), the following predictions can be made, for 10 mM TMA. An apparent opening would consist of a burst of roughly 280 very brief openings and blockages, each with mean duration about 1.5 μs . Filtering would make this look like a single opening with half the true amplitude. All the blockages would be too short to be resolved (less than a 1 in 10^6 chance of any blockage being resolved in an apparent opening, with a resolution of 30 μs).

We therefore attempted fits that assumed very fast selective open-channel block. When the transition rates between two (or more) states are very fast then the states can be pooled into a single compound state for the purposes of kinetics. In this case the open and blocked states, A_2R^* and A_2R^*B , are pooled. This has the effect of making the shutting rate α_2 appear to be concentration-dependent. Therefore α_2 is replaced for all calculations by $\alpha_2/(1 + [B]/K_B)$, because the fraction of the time for which the compound state is not blocked, and therefore available to shut, is

$1/(1 + [B]/K_B)$ where $[B]$ is the blocker (agonist) concentration. The rates of block and unblock do not appear in this, but only the equilibrium constant for block, because of the assumption that these rates are so fast that the blocking reaction is at equilibrium throughout. We found that fits with the fast block correction (not shown) were somewhat less good than those without it. This suggests that TMA is not a pure open channel blocker⁷. If it were, we would also expect that at a concentration of K_B (about 10 mM) the length of the apparent opening would be doubled⁸. We failed to observe this lengthening, presumably because the TMA-blocked channel can shut^{9,10}. The fits in Figure 5 and Supplementary Figure 4 were done without the fast block correction. It is important to note that both fits gave the same qualitative result, namely that partial agonism depends mainly on poor flipping rather than inefficient opening.

Extended discussion of results

Agonist affinity for the open states

Dissociation of agonist from open states must, in principle, be possible so it may be asked why the open states are not connected in the flip mechanism (Figs. 2a and 5a). The main reason is that dissociation appears to be too slow to be detected⁶, and it is not sensible to include in the fitting process parameters that cannot be estimated reliably from the data. If the open states are joined, then new cycles are created, and if these cycles are assumed to obey microscopic reversibility, then this places an extra constraint on the mechanism. In the case of the glycine receptor, this constraint would mean, for example, that the ratio of the open-shut equilibrium constant for triply- and doubly-occupied receptors (E_3/E_2) should be the same as the ratio for doubly- and singly-occupied

receptors (E_2/E_1). These ratios were not found to be the same⁶, so the extra constraint produced by joining the open states actually reduced somewhat the quality of the fit. This could be a result of the flip mechanism being still not sufficiently detailed. It might also result from there being some interaction between ion flow and the open-shut conformation change that results in a breach of microscopic reversibility. This is an interesting question for future investigation, but it does not affect the conclusions of this paper.

Fits for the heteromeric glycine receptor

Supplementary Table 1 shows the complete results of the global fits to sets of observations with glycine and taurine. It was not possible to use taurine concentrations lower than 1 mM because openings were sparse and occurred in short bursts. Many bursts were so short that heteromeric and homomeric openings could not be distinguished unambiguously. So it is not surprising that initial fits suggested that there were few monoliganded openings in our records. Therefore monoliganded flipped and open states were not included in the mechanism in the final fits (Fig. 2a, grey regions).

With glycine as agonist, all 12 free rate constants are quite well determined. With taurine as agonist, the rates for the triliganded receptor are also quite precise, but those for the diliganded receptor are less precise. That is because it was necessary to limit our fits to high concentrations of taurine (1 mM and higher), and calculations with the fitted rate constants suggest that most receptors will be triliganded even at 1 mM. This is confirmed in Supplementary Figure 1, which completes the display of the global fitting of the taurine data shown in Figure 2 of the paper. The conditional mean open time shows little dependence on adjacent shut time, as expected if most receptors are fully liganded, and this outcome is predicted by the calculated conditional means calculated from the fitted rate constants (open symbols and dashed lines).

The value of γ_2 is faster than we can expect to estimate; this value is determined by microscopic reversibility and all that can be said is that the lifetime of the diliganded flipped conformation appears to be very small. This outcome is not at all critical for our conclusions, which depend on the properties of the fully-liganded receptor.

The values in Supplementary Table 1 give the basis for the conclusion (main paper) that the affinities of glycine and taurine for the resting state (K) are comparable, but that the affinity of taurine for the flipped state (K_F) is much lower than that of glycine. This accounts (via microscopic

reversibility) for the finding that the flipping equilibrium constant, F_3 , is very much smaller for taurine than for glycine. The flipping equilibrium constant is smaller for taurine than glycine by a factor of about 180, both because the rate of entry into the flipped state (δ_3) is slower (by a factor of 28) and because the rate of return to the resting conformation (γ_3) is faster (by a factor of about 6). The reason for the higher affinity of glycine for the flipped conformation is that the association rate constant for glycine (k_{F+}), $1.50 \times 10^8 \text{ M}^{-1}\text{s}^{-1}$, is almost 63 times faster than that for taurine.

Fits for the nicotinic receptor

The complete numerical results for fits with acetylcholine and with TMA at both -80 mV and at $+80 \text{ mV}$ are shown in Supplementary Table 2. The tests for the quality of the fits are shown in Supplementary Figures 2 - 5. These Figures show the apparent open and shut times distributions that are predicted by the fit, superimposed on histograms of the observations, for each of the concentrations in one of the sets of data that contributes to the averages in the Tables (the P_{open} curves that are predicted by the fit are shown in the main paper, and are seen to describe the observations well). The Supplementary Figures show also the predicted and observed conditional mean open time plots, as described in the legend of Supplementary Figure 1. The flatness of most of these plots suggests, as for the glycine receptor experiments, that most receptors are fully liganded under the conditions we use. It is, therefore, not surprising that the rate constants for monoliganded receptors are less precise than those for diliganded receptors. This is of secondary importance because it is the latter than we need to test our hypothesis.

The fits for ACh at -100 mV (Supplementary Fig. 2) are excellent at all concentrations. Records with ACh have not previously been fitted with the flip model. The values of the open-shut equilibrium constant, E_2 , are very similar for ACh and for TMA at both negative and positive membrane potentials, as are the underlying rate constants. But the flipping equilibrium constant, F_2 , for the partial agonist, TMA, is smaller than that for ACh by a factor of 27 (at negative potentials) or 18 (at positive potential), again largely as a result of the transition from resting to flipped being slower for TMA than for ACh. The gating constant, E_2 , is reduced at $+80 \text{ mV}$ by about the amount (69 mV for e -fold change) expected from the voltage dependence of the opening and shutting rates, but the flipping equilibrium constant is reduced too, and remains much (47-fold) smaller than the open-shut equilibrium constant. This provides confirmation of our thesis that partial agonism is a property of the flipping step rather than the open-shut conformation change step, under conditions where the result is unaffected by the powerful channel block produced by agonist at negative membrane potentials.

Results with ACh can usually be fitted quite well with the assumption that the binding sites are independent. The two sites are certainly physically different, though reports about the extent to which this is detectable with ACh itself are quite inconsistent. In any case, ACh does not show the strong apparent interaction between binding sites that provided the initial incentive to develop the flip mechanism for glycine receptors⁶. This is borne out by the finding that ACh (unlike glycine) has only a slightly higher affinity for the flipped conformation than for the resting state (Supplementary Table 2).

The fits for the acetylcholine records at positive membrane potential (Supplementary Fig. 3) are reasonably good at all concentrations. However, it should be mentioned that the single-channel activations by ACh at +80 mV were difficult to idealise unambiguously, especially at the higher ACh concentration. In these records, activations occurred as barrages of short openings and shuttings (see the bottom trace in Supplementary Fig. 3a), which were mostly too short at our bandwidth to reach the full open or full shut level. Because of this, we imposed on the acetylcholine records at +80 mV a much more conservative resolution of 100 μ s. We were concerned that including these records would lead to inaccuracy in the estimation of rate constants. However, we found that the coefficients of variation of the rate constant estimates were still reasonably low (see Supplementary Table 2). In addition to that, we also measured the P_{open} by integration of the raw data trace, a method that needs only an estimate of channel amplitude, but which is independent of idealisation and of filtering. These P_{open} values were similar to those measured by idealisation. Furthermore, the reduction of the maximum P_{open} at positive potentials is similar to that reported previously¹¹ (for frog muscle). The predictions of the fits of the flip model described satisfactorily the experimental observations, including the P_{open} curve, in which open probabilities were estimated independently of the idealisation method. This encourages us to trust the results, though they cannot be quite as reliable as those at negative potentials. The results were very similar to those at negative potentials.

One interesting aspect of the results in Supplementary Table 2 is that the main channel opening rate, β_2 , seems to be almost as voltage-dependent as the shutting rate, α_2 for both ACh and TMA. Previous reports^{12,13} have suggested that the opening rate is almost independent of membrane potential, whereas the shutting rate, α_2 , increases strongly with depolarisation, changing e -fold for each 55 – 80 mV. The voltage dependence of the overall resting-open transition also has a contribution from the flipping rate constants which change with voltage in the same direction, but to

a lesser extent than the open-shut rates constants. Insofar as our mechanism describes reality better than those used before, it may be that these are better estimates of the true rate constants.

Implications of the results for the rise time of macroscopic responses

The existence of an intermediate shut state of the fully-occupied receptor, the flip state, must inevitably slow the rise time of the response to a step to a large agonist concentration, including the rise time of synaptic currents. It is important to be sure that the predictions of the flip model are consistent with what is known about response rise times.

In the case of the glycine receptor, it was shown by Burzomato *et al.* (2004)⁶ that the rate constants inferred from single channel analysis predicted accurately the shape of miniature synaptic currents mediated by glycine in rat spinal motor neurones. In contrast, responses to fast concentration jumps on outside-out patches were rather faster than predicted from recordings in the cell-attached mode and this appears to be an artefact of patch excision (Pitt *et al.*, submitted).

There have been many more estimates of rise time for the muscle type nicotinic receptor than for the glycine receptor. Most estimates of the fully-liganded opening rate constant, β_2 , are in the range 40,000 to 80,000 s⁻¹¹⁴⁻¹⁷. Our estimate of β_2 in the context of the flip mechanism is very similar to that estimated from the fastest concentration jumps by Maconochie and Steinbach (1998)¹⁵. Because of the presence of the flip state, our prediction for the rise time of the response to high concentrations is slower.

Simulated concentration jump responses using our estimates of flipping and open-shut rate constants give rise time constant values between 40 and 70 μ s for ACh. This prediction is close to the mean first passage time from the fully-liganded resting state (A₂R) to the open state, as expected when high concentration makes binding very fast. This mean first passage time can be calculated from equation 3.91 of Colquhoun & Hawkes (1982)¹⁸ by substitution of the appropriate initial vector in place of the equilibrium vector, ϕ_s . This rise time prediction is still quite fast enough to be consistent with even the fastest estimates of the rise times of miniature synaptic currents¹⁹, and with most concentration jump experiments too. It is slower than would be expected from the fastest jump experiments¹⁵. This could be a consequence of artefactual speeding of the response when outside-out patches are excised (as seen with the glycine receptor), or simply a consequence of the fact that we are using the human receptor rather than the mouse receptor.

Φ value analysis

The technique of rate-equilibrium free energy relationship analysis²⁰ can be applied to single channel data in order to obtain information on the relative timing of movements for the different parts of the channel²¹⁻²³. In the first application of this technique to channels, Grosman *et al.* (2000)²¹ investigated the resting-open reaction of the fully-liganded muscle nicotinic channel by activating it by a series of agonists. They found a high Φ value (0.93). This result was interpreted as meaning that the area perturbed by the experimental manipulation (i.e. the ligand binding site) moved very early in the chain of movements that convert binding to opening^{22,23}.

The mechanisms that we fitted are more detailed than that used in the original Φ value analysis, as they include three distinguishable states for the saturated receptor (resting, flipped and open; Fig. 3) rather than two (resting and open). It is possible that our flipped state represents a particularly stable reaction intermediate among the microstates that are thought to populate the flattish, rugged energy landscape at the transition state²⁴. Presumably the flip state would correspond to the first of the five blocks of amino acids that Auerbach's group²⁵ identifies, or the first state in rapid equilibrium with one or more of the following intermediates.

In order to calculate the Φ value for the agonist perturbation in the glycine channel in a manner comparable to that of Grosman *et al.* (2000)²¹, we have to obtain both the effective forward rate and the effective equilibrium constant for the whole transition between resting and open (denoted β_{eff} and E_{eff}), from the results of our fits for the two agonists. When our system is reduced to two states, shut and open, the effective equilibrium constant is $E_{\text{eff}} = EF/(1 + F)$ where E and F refer to the fully-liganded receptor. This must be equal to $\beta_{\text{eff}}/\alpha$ so the effective opening rate constant is

$$\beta_{\text{eff}} = \beta \left(\frac{F}{1 + F} \right)$$

This is easily shown to be the high-concentration limit of the reciprocal of the mean of all shut times, as calculated from Equation 3.91 of Colquhoun & Hawkes, 1982¹⁸.

With these results we can calculate Φ values as the slope of the graph of $\log(\beta_{\text{eff}})$ against $\log(E_{\text{eff}})$, by least squares fit of a straight line to the two groups of points from replicate experiments with taurine and glycine. We obtained a Φ value of 0.71 ± 0.06 ($n = 3$ replicate experiments for both glycine and taurine), somewhat smaller than the value of 0.93 reported by Grosman *et al.* (2000)²¹ with a large series of agonists on the nicotinic channel. This is because the change in E_{eff} was in part due to a change in the shutting rate constant for the fully liganded receptor, α . We found a

modest, but consistent, difference in α_3 between glycine and taurine by a factor of about 2 on average (Supplementary Table 1) and this is sufficient to reduce Φ below 1.

When the same procedure was repeated for the nicotinic receptor with acetylcholine and TMA, we obtained Φ values very close to unity, entirely consistent with those reported by Grosman *et al.* (2000)²¹. We found $\Phi = 1.02 \pm 0.06$ at negative membrane potentials ($n = 3$ replicate experiments for both agonists) and 1.02 ± 0.08 at positive potentials ($n = 2$ replicates). This suggests that, in the case of the nicotinic receptor, the flip state is likely to be a direct physical manifestation of sojourns the first block of amino acids to move during activation as postulated by Chakrapani *et al.* (2004)²⁶.

Supplementary information- References

1. Groot-Kormelink, P. J., Beato, M., Finotti, C., Harvey, R. J. & Sivilotti, L. G. Achieving optimal expression for single channel recording: a plasmid ratio approach to the expression of $\alpha 1$ glycine receptors in HEK293 cells. *J. Neurosci. Meth.* **113**, 207-214 (2002).
2. Burzomato, V., Groot-Kormelink, P. J., Sivilotti, L. G. & Beato, M. Stoichiometry of recombinant heteromeric glycine receptors revealed by a pore-lining region point mutation. *Recept. Chann.* **9**, 353-361 (2003).
3. Bormann, J., Rundström, N., Betz, H. & Langosch, D. Residues within transmembrane segment M2 determine chloride conductance of glycine receptor homo- and hetero-oligomers. *EMBO J.* **12**, 3729-3737 (1993).
4. Beato, M., Groot-Kormelink, P. J., Colquhoun, D. & Sivilotti, L. G. Openings of the rat recombinant $\alpha 1$ homomeric glycine receptor as a function of the number of agonist molecules bound. *J. Gen. Physiol.* **119**, 443-466 (2002).
5. Thomas, P. & Smart, T. G. HEK293 cell line: a vehicle for the expression of recombinant proteins. *J. Pharmacol. Toxicol. Methods* **51**, 187-200 (2005).
6. Burzomato, V., Beato, M., Groot-Kormelink, P. J., Colquhoun, D. & Sivilotti, L. G. Single-channel behavior of heteromeric $\alpha 1\beta$ glycine receptors: an attempt to detect a conformational change before the channel opens. *J. Neurosci.* **24**, 10924-10940 (2004).
7. Akk, G. & Steinbach, J. H. Activation and block of mouse muscle-type nicotinic receptors by tetraethylammonium. *J. Physiol* **551**, 155-168 (2003).
8. Neher, E. & Steinbach, J. H. Local anaesthetics transiently block currents through single acetylcholine-receptor channels. *J. Physiol. (Lond.)* **277**, 153-176 (1978).
9. Lingle, C. Blockade of cholinergic channels by chlorisondamine on a crustacean muscle. *J. Physiol. (Lond.)* **339**, 395-417 (1983).
10. Gurney, A. M. & Rang, H. P. The channel-blocking action of methonium compounds on rat submandibular ganglion cells. *Br. J. Pharmacol.* **120**, 471-490 (1984).
11. Colquhoun, D. & Ogden, D. C. Activation of ion channels in the frog end-plate by high concentrations of acetylcholine. *J. Physiol. (Lond.)* **395**, 131-159 (1988).
12. Colquhoun, D. & Sakmann, B. Fast events in single-channel currents activated by acetylcholine and its analogues at the frog muscle end-plate. *J. Physiol. (Lond.)* **369**, 501-557 (1985).
13. Auerbach, A., Sigurdson, W., Chen, J. & Akk, G. Voltage dependence of mouse acetylcholine receptor gating: different charge movements in di-, mono- and unliganded receptors. *J. Physiol. (Lond.)* **494 (Pt 1)**, 155-170 (1996).
14. Sine, S. M. & Steinbach, J. H. Activation of acetylcholine receptors on clonal mammalian BC3H-1 cells by high concentrations of agonist. *J. Physiol. (Lond.)* **385**, 325-359 (1987).

15. Maconochie, D. J. & Steinbach, J. H. The channel opening rate of adult- and fetal-type mouse muscle nicotinic receptors activated by acetylcholine. *J. Physiol. (Lond.)* **506**, 53-72 (1998).
16. Hatton, C. J., Shelley, C., Brydson, M., Beeson, D. & Colquhoun, D. Properties of the human muscle nicotinic receptor, and of the slow-channel myasthenic syndrome mutant epsilonL221F, inferred from maximum likelihood fits. *J. Physiol. (Lond.)* **547**, 729-760 (2003).
17. Salamone, F. N., Zhou, M. & Auerbach, A. A re-examination of adult mouse nicotinic acetylcholine receptor channel activation kinetics. *J. Physiol. (Lond.)* **516**, 315-330 (1999).
18. Colquhoun, D. & Hawkes, A. G. On the stochastic properties of bursts of single ion channel openings and of clusters of bursts. *Phil. Trans. R. Soc. Lond. B* **300**, 1-59 (1982).
19. Stiles, J. R., Van, H. D., Bartol, T. M., Jr., Salpeter, E. E. & Salpeter, M. M. Miniature endplate current rise times less than 100 μ s from improved dual recordings can be modeled with passive acetylcholine diffusion from a synaptic vesicle. *Proc. Natl. Acad. Sci. U. S. A* **93**, 5747-5752 (1996).
20. Fersht, A. R. Relationship of Leffler (Bronsted) α values and protein folding Φ values to position of transition-state structures on reaction coordinates. *Proc. Natl. Acad. Sci. U. S. A.* **101**, 14338-14342 (2004).
21. Grosman, C., Zhou, M. & Auerbach, A. Mapping the conformational wave of acetylcholine receptor channel gating. *Nature* **403**, 773-776 (2000).
22. Zhou, Y., Pearson, J. E. & Auerbach, A. Φ -value analysis of a linear, sequential reaction mechanism: theory and application to ion channel gating. *Biophys. J.* **89**, 3680-3685 (2005).
23. Auerbach, A. How to turn the reaction coordinate into time. *J. Gen. Physiol* **130**, 543-546 (2007).
24. Auerbach, A. Gating of acetylcholine receptor channels: brownian motion across a broad transition state. *Proc. Natl. Acad. Sci. U. S. A.* **102**, 1408-1412 (2005).
25. Purohit, P., Mitra, A. & Auerbach, A. A stepwise mechanism for acetylcholine receptor channel gating. *Nature* **446**, 930-933 (2007).
26. Chakrapani, S., Bailey, T. D. & Auerbach, A. Gating dynamics of the acetylcholine receptor extracellular domain. *J. Gen. Physiol.* **123**, 341-356 (2004).
27. Colquhoun, D., Dowsland, K. A., Beato, M. & Plested, A. J. How to impose microscopic reversibility in complex reaction mechanisms. *Biophys. J.* **86**, 3510-3518 (2004).

Supplementary Tables 1 and 2

The values shown are the estimates of the rate constants from the fits of mechanisms shown in Figure 2 and Supplementary Figure 1 (taurine), Figure 5 and Supplementary Figures 4 and 5 (TMA -80 mV and +80 mV) and Supplementary Figures 2 and 3 (ACh -100 mV and +80 mV, respectively). The names of the rate constants are as shown in the state diagrams in the Figures. Values for glycine, shown for reference, are from Burzomato *et al.*, 2004¹².

Values shown are the averages of the rate constant estimates obtained from fits to several independent data sets, three each for taurine, ACh and TMA at negative potential and two each for ACh and TMA at positive potentials, together with the error in the estimates, expressed as coefficient of variation (right hand columns). Each set contained patches at three different agonist concentrations (four for glycine and ACh): 1 to 100 mM for taurine; 10, 30, 100, and 1,000 μ M for glycine; 0.05 to 64 μ M for ACh at -100 mV; 3 to 300 μ M for ACh at +80 mV; 0.1 to 30 mM for TMA at -80 mV; 0.3 to 100 mM for TMA at +80 mV. Equilibrium constants were calculated separately as the ratios of the appropriate rate constants in each of the replicate sets and the individual equilibrium constants were then averaged.

All rate constants were fitted freely, except for the constraint for microscopic reversibility imposed by the presence of cycles in the mechanisms (see Colquhoun *et al.*, 2004²⁷).

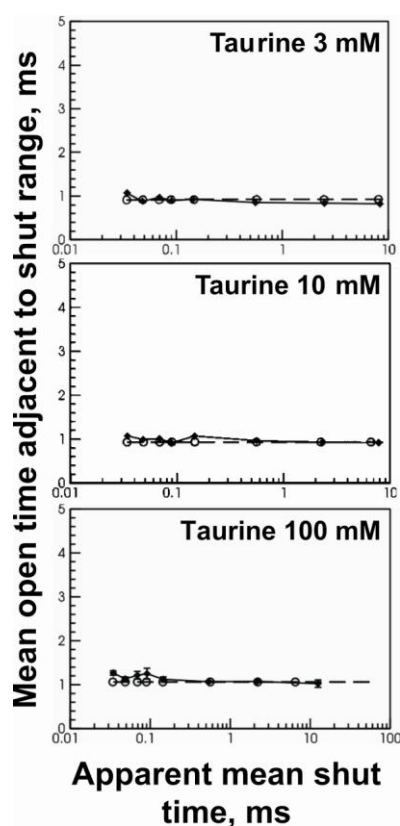
Supplementary Table 1. Fitted rate constants for the glycine receptor.

Rate constant	Units	Glycine		Taurine	
α_2	s^{-1}	2,100	$\pm 12\%$	1,150	$\pm 61\%$
β_2	s^{-1}	28,000	$\pm 17\%$	250	$\pm 92\%$
α_3	s^{-1}	7,000	$\pm 18\%$	14,500	$\pm 7\%$
β_3	s^{-1}	129,000	$\pm 4\%$	133,000	$\pm 3\%$
γ_2	s^{-1}	18,000	$\pm 14\%$	739,000	$\pm 35\%$
δ_2	s^{-1}	6,800	$\pm 6\%$	96,000	$\pm 71\%$
γ_3	s^{-1}	900	$\pm 26\%$	5,170	$\pm 11\%$
δ_3	s^{-1}	20,900	$\pm 3\%$	740	$\pm 10\%$
k_{F+}	$M^{-1} s^{-1}$	1.50×10^8	$\pm 5\%$	2.38×10^6	$\pm 47\%$
k_{F-}	s^{-1}	1,200	$\pm 12\%$	1,230	$\pm 21\%$
$k_{-1} = k_{-2} = k_{-3}$	s^{-1}	300	$\pm 6\%$	220	$\pm 19\%$
$k_{+1} = k_{+2} = k_{+3}$	$M^{-1} s^{-1}$	5.9×10^5	$\pm 6\%$	2.2×10^5	$\pm 20\%$
$E_2 (= \beta_2/\alpha_2)$	-	13	$\pm 9\%$	0.14	$\pm 56\%$
$E_3 (= \beta_3/\alpha_3)$		20	$\pm 16\%$	9.2	$\pm 3\%$
$F_2 (= \delta_2/\gamma_2)$	-	0.4	$\pm 15\%$	0.12	$\pm 51\%$
$F_3 (= \delta_3/\gamma_3)$	-	27	$\pm 31\%$	0.15	$\pm 20\%$
$K (= k_{-1}/k_{+1})$	μM	520	$\pm 12\%$	1,040	$\pm 16\%$
$K_F (= k_{F-}/k_{F+})$	μM	8	$\pm 14\%$	690	$\pm 27\%$

Supplementary Table 2. Fitted rate constants for the nicotinic acetylcholine receptor.

Rate constant	Units	ACh; -100 mV		ACh; +80 mV		TMA; -80 mV		TMA; +80 mV	
α_1	s^{-1}	17,700	$\pm 24\%$	12,200	$\pm 21\%$	330	$\pm 97\%$	830	$\pm 93\%$
β_1	s^{-1}	40	$\pm 88\%$	54,000	$\pm 24\%$	2	$\pm 42\%$	2	$\pm 49\%$
α_2	s^{-1}	2,560	$\pm 5\%$	9,550	$\pm 11\%$	2,520	$\pm 12\%$	9,100	$\pm 15\%$
β_2	s^{-1}	87,700	$\pm 3\%$	29,400	$\pm 4\%$	70,500	$\pm 9\%$	25,000	$\pm 3\%$
γ_1	s^{-1}	128,000	$\pm 98\%$	929,000	$\pm 5\%$	146,000	$\pm 71\%$	180,000	$\pm 89\%$
δ_1	s^{-1}	295,000	$\pm 96\%$	2,990	$\pm 21\%$	540	$\pm 98\%$	5,700	$\pm 87\%$
γ_2	s^{-1}	8,400	$\pm 54\%$	16,100	$\pm 19\%$	12,600	$\pm 25\%$	19,900	$\pm 8\%$
δ_2	s^{-1}	22,900	$\pm 22\%$	16,900	$\pm 21\%$	1,470	$\pm 27\%$	1,200	$\pm 19\%$
k_{F+}	$M^{-1} s^{-1}$	2.03×10^8	$\pm 26\%$	8.43×10^8	$\pm 18\%$	2.90×10^8	$\pm 68\%$	4.1×10^6	$\pm 11\%$
k_{F-}	s^{-1}	3,240	$\pm 39\%$	108	$\pm 2\%$	15,500	$\pm 32\%$	4,900	$\pm 7\%$
$k_{-1} = k_{-2}$	s^{-1}	9,480	$\pm 48\%$	27,900	$\pm 21\%$	9,730	$\pm 30\%$	1,800	$\pm 48\%$
$k_{+1} = k_{+2}$	$M^{-1} s^{-1}$	2.71×10^8	$\pm 59\%$	6.51×10^8	$\pm 25\%$	5.65×10^6	$\pm 56\%$	7.4×10^5	$\pm 30\%$
k_{+B}	$M^{-1} s^{-1}$	8.6×10^7	$\pm 14\%$	-	-	-	-	-	-
k_{-B}	s^{-1}	95,300	$\pm 3\%$	-	-	-	-	-	-
$E_1 (= \beta_1/\alpha_1)$	-	0.038	$\pm 94\%$	4.4	$\pm 3\%$	0.046	$\pm 81\%$	0.020	$\pm 98\%$
$E_2 (= \beta_2/\alpha_2)$		34.4	$\pm 5\%$	3.1	$\pm 15\%$	28.1	$\pm 2\%$	2.8	$\pm 12\%$
$F_1 (= \delta_1/\gamma_1)$	-	2.3	$\pm 55\%$	0.003	$\pm 27\%$	0.014	$\pm 79\%$	0.03	$\pm 7\%$
$F_2 (= \delta_2/\gamma_2)$	-	3.8	$\pm 27\%$	1.1	$\pm 2\%$	0.14	$\pm 40\%$	0.06	$\pm 11\%$
$K (= k_{-1}/k_{+1})$	μM	40.1	$\pm 13\%$	43	$\pm 5\%$	3,000	$\pm 40\%$	2,310	$\pm 21\%$
$K_F (= k_{F-}/k_{F+})$	μM	20.7	$\pm 46\%$	0.13	$\pm 21\%$	340	$\pm 83\%$	1,240	$\pm 18\%$
$K_B (= k_{-B}/k_{+B})$	mM	1.2	$\pm 18\%$	-	-	-	-	-	-

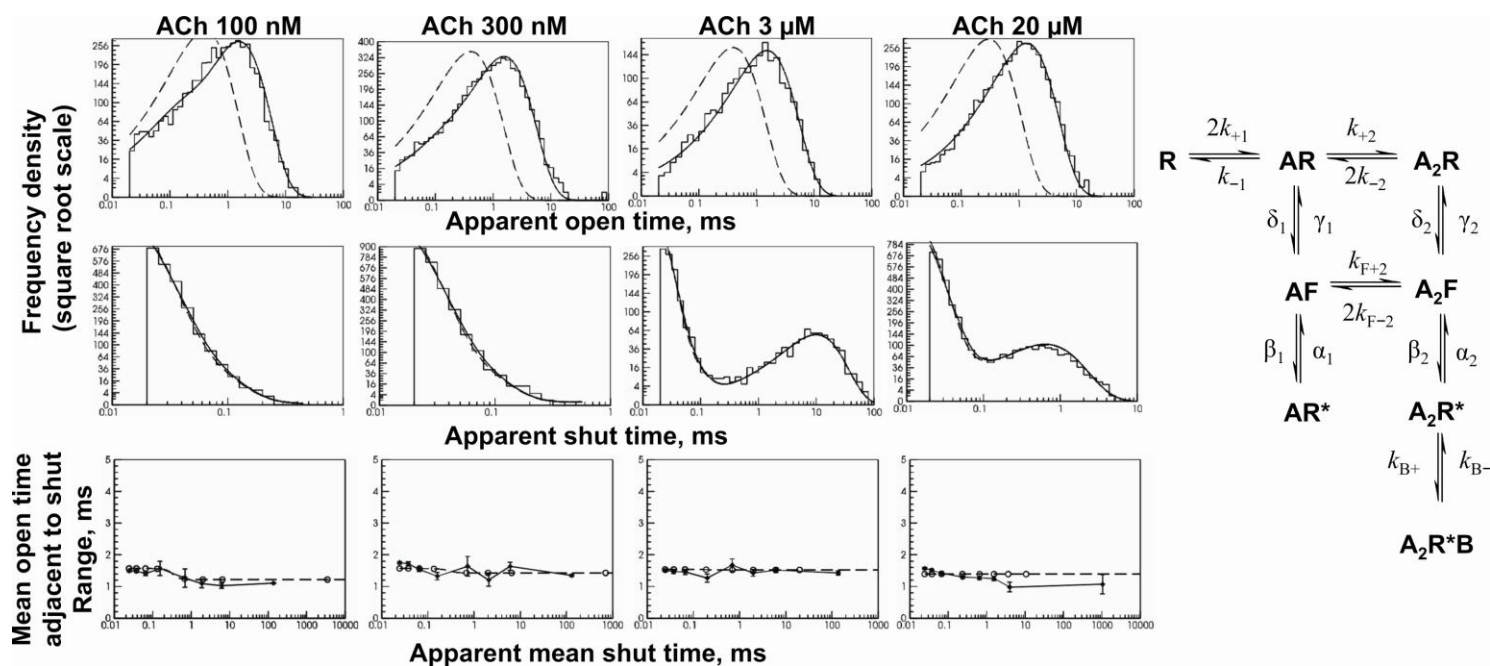
Supplementary Figure 1.



The observed lack of correlation between adjacent open and shut times is predicted well by the fit of the taurine data.

The plots show as filled symbols the mean apparent duration of openings that were adjacent to shut times in a specified range. The open symbols and the dashed lines are the predictions of the fitted model. The prediction agrees reasonably well with the experimental points. These plots illustrate the correlation between the adjacent open and shut times. Apparently, there is little such correlation in records of taurine-bound glycine receptor activations in the range of concentrations between 3 to 100 mM, as mean apparent open times are approximately 1 ms, irrespective of whether they are near a short shutting (points on the left) or a long one. This is because of the paucity of openings from receptors that are less than triply-liganded.

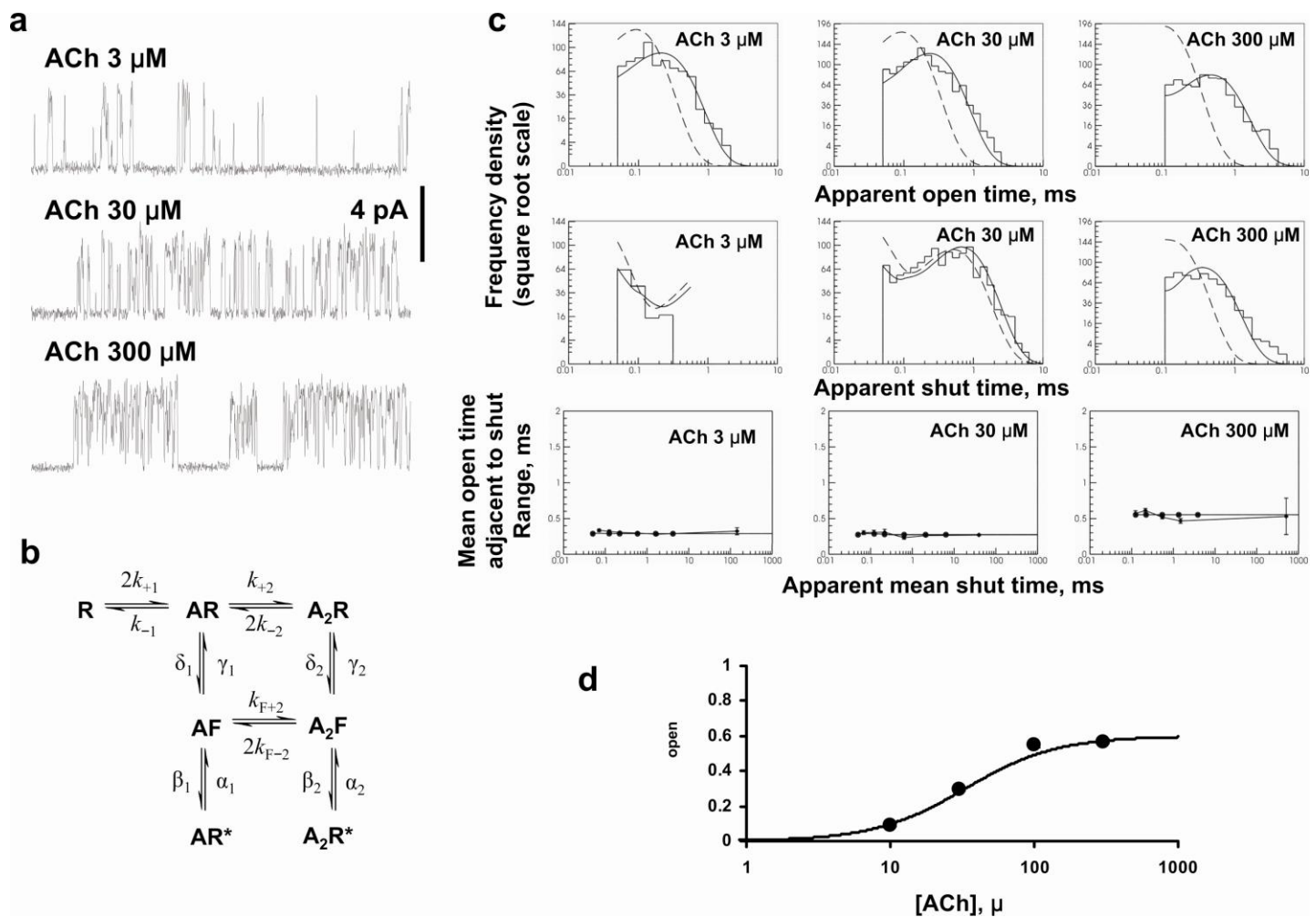
Supplementary Figure 2.



The ‘flip’ mechanism describes well channel activations evoked by a range of ACh concentrations at -100 mV. The mechanism is shown on the right and explicitly includes a blocked state, linked to the diliganded open state.

The plots show the experimental apparent open (top row) and shut (middle row) time distributions (stepwise lines) at four ACh concentrations (0.1, 0.3, 3 and 20 μM). The frequency densities for the distributions of apparent dwell times calculated from the fitted rate constants at our experimental resolution are the solid lines superimposed to the data histograms. The dashed lines are the distributions predicted if resolution were perfect and no events were missed. The difference between the two shows how essential it is to have full missed event correction in the fitting process, particularly for open times. The bottom row of graphs show the mean apparent duration of openings that were adjacent to shut times in a specified range (filled symbols). The predictions of the fitted model are shown as open symbols and dashed lines.

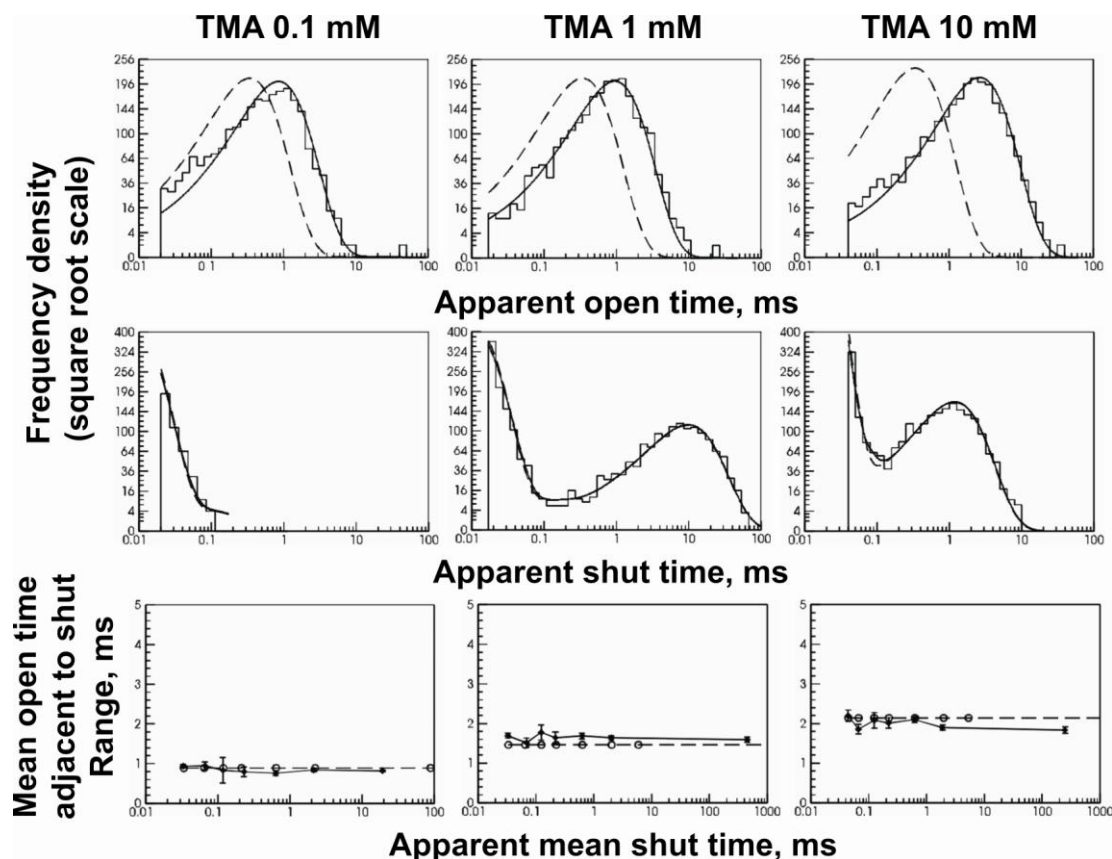
Supplementary Figure 3.



The results of the maximum likelihood fit of the ‘flip’ mechanism to the openings of the nicotinic receptor activated by ACh recorded at +80 mV.

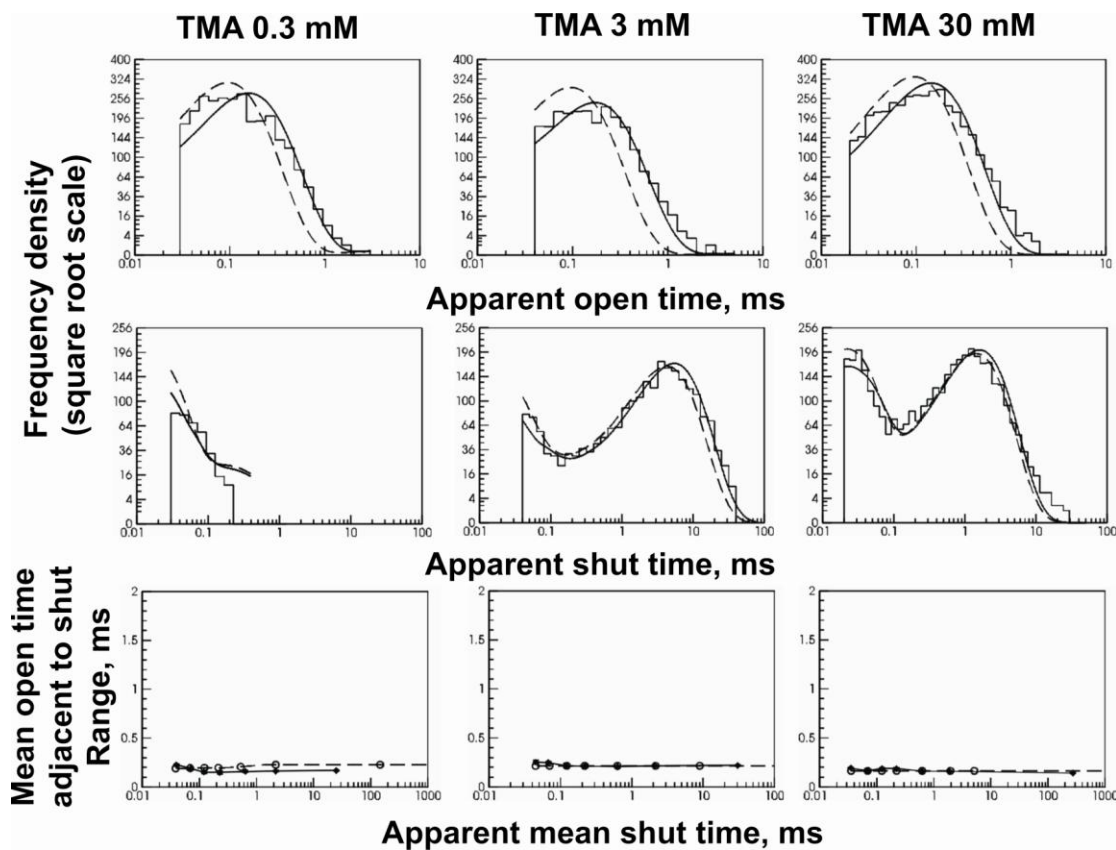
a, Single-channel currents (opening upwards) produced by increasing concentrations of ACh at +80 mV transmembrane potential. At high concentrations, activations become more closely spaced, and open probability increases. b, Mechanism fitted to nicotinic receptor activations by ACh at +80 mV. c, The plots show the experimental apparent open (top row) and shut (middle row) time distributions (stepwise lines) at three ACh concentrations (3, 30 and 300 μM), together with the predictions of the fit (details as in Supplementary Figure 2). d, The results of the fit predict accurately the channel open probability.

Supplementary Figure 4.



The complete results of the maximum likelihood fit of the 'flip' mechanism to the idealised records of openings of the nicotinic receptor activated by TMA at -80 mV. Same set and mechanism as in Figure 5c: all distributions and plots are shown here, better to allow a judgement of the quality of the global fit. The top and middle rows are distributions of apparent open and shut times (see legend to Supplementary Figure 2) and the bottom row are correlation plots (see legend to Supplementary Figure 1).

Supplementary Figure 5.



The complete results of the maximum likelihood fit of the 'flip' mechanism to the openings of the nicotinic receptor activated by TMA recorded at +80 mV. Same sets and mechanism as in Figure 5d: all distributions and plots are shown here, better to allow a judgement of the quality of the global fit. The top and middle rows are distributions of apparent open and shut times (see legend to Supplementary Figure 2) and the bottom row are conditional mean apparent open time plots (see legend to Supplementary Figure 1).